EnvironmentAsia
The international journal by the Thai Society of Higher Education Institutes on Environment

EnvironmentAsia 17(3) 2024 162-173
DOI 10.14456/ea.2024.44
ISSN 1906-1714; ONLINE ISSN: 2586-8861

Investigation of Composites Reinforced with *Salacca zalacca* Midrib Fiber and Microcrystalline Cellulose as Prosthetic Sockets Materials

Sakuri Sakuri[1*], Bambang Sugiantoro[1], Haryanto Haryanto[2], and Reza Azizul Nasa Al Hakim[3]

[1] *Department of Mechanical Engineering STT Wiworotomo, Purwokerto, Indonesia*
[2] *Department of Chemical Engineering, Muhammadiyah University, Purwokerto, Indonesia*
[3] *Department of Industrial Engineering Jendral Soedirman University, Purwokerto, Indonesia*

*Corresponding author: sakuridahlan@stt-wiworotomo.ac.id
Received: March 3, 2024; Revised: April 5, 2024; Accepted: June 11, 2024

Abstract

This study aimed to determine the effect of alkaline treatment on *Salacca zalacca* midrib fiber (ZMF) in terms of fiber density, crystallinity index, thermal stability, scanning electron microscopy (SEM), interfacial share strength (IFSS), water absorption, tensile and flexural strength of composites. The mechanical properties of composites enriched with microcrystalline cellulose (MCC) as prosthetic sockets materials were also assessed. During the procedures, ZMF was removed from the stem and soaked in 5% sodium hydroxide for 3, 6, 9, and 12 hours. Subsequently, composites materials were molded by mixing with 10% MCC under controlled conditions of 150 rpm rotation speed, temperature 40 °C, and 30 minutes mixing duration. The results showed that alkaline treatment yielded several favorable outcomes, including improved particle bonding, increased thermal compatibility, and a cleaner fiber surface due to the reduction of hemicellulose, lignin, pectin, and other impurities. In addition, the incorporation of MCC into composites increased their tensile and flexural strength. The water absorption test showed that the treated fiber had a lower absorption rate.

Keywords: Midrib fiber; Microcrystalline cellulose; Mechanical properties; Composite fiber; Prosthetic socket

1. Introduction

Natural fiber is widely used in the production of prosthetic sockets due to its biodegradability, environmental friendliness, unlimited availability, cost-effectiveness, high strength, and excellent mechanical resistance. (Sakuri *et al.,* 2020a). Several studies have explored the use of natural fiber, such as hemp, banana (Seal *et al.,* 2023), cotton (Oleiwi *et al.,* 2023), and cantala fiber (Sakuri *et al.,* 2023). Despite the potential, various limitations have been identified, including low tensile strength, flexural strength, and modulus of elasticity compared to carbon and glass. Therefore, this current study aims to address the limitations by focusing on the development of prosthetic sockets through the reinforcement of *Salacca zalacca* midrib fiber (ZMF) with microcrystalline cellulose (MCC). The primary objective is to enhance the tensile strength, flexibility, and modulus of elasticity.

According to previous reports, *Salacca zalacca* plant is often found in various regions in Indonesia, including Jakarta, Central Java, West Java, West Nusa Tenggara, Maluku, Kalimantan, Bali, Sulawesi, and Yogyakarta. The midrib fiber (ZMF) of the plant has been

reported to possess various applications but remains underutilized. ZMF typically contains 44.87% alpha-cellulose, 35.84% hemicellulose, and amorphous (Hakim *et al.,* 2022). In addition, its use as a substitute for synthetic fiber has attracted significant attention due to various advantages, such as unlimited availability, biodegradability, and high toughness (Ilyas *et al.,* 2022).

The drawbacks associated with ZMF as a natural fiber include its high polarity, non-abrasive qualities, and lack of compatibility with polymers (Ariawan *et al.,* 2020). To address these drawbacks, various approaches have been explored to improve the properties. The approaches include the use of fumigation, alkali (Sakuri *et al.,* 2020b), silane, and permanganate treatment (Ihueze *et al.,* 2021). Alkaline treatment has proven effective in improving the bonding between cantala fiber and unsaturated polyester, thereby increasing the strength of prosthetic sockets composites (He *et al.,* 2021). In addition, surface modification can increase the wetting of fiber with the matrix, leading to improved mechanical properties between banana coir and the matrix in automotive applications (Wang *et al.,* 2021). The addition of MCC to unsaturated polyester has also been shown to increase tensile strength, bending, and elastic modulus (Sakuri *et al.,* 2020b).

In line with previous reports, alkaline treatment can enhance the interfacial bond between fiber and the matrix by roughening the surface through the removal of amorphous elements, such as pectin, lignin, and hemicellulose, leading to improved mechanical properties (Sakuri *et al.,* 2020c). The addition of MCC to the matrix has the potential to increase the tensile strength and elastic modulus. MCC typically comprises pure cellulose particles that are micro-sized and can effectively fill holes in composites (Hafidz *et al.,* 2022). The material can also increase thermal stability, reduce the coefficient of thermal expansion, lead to clearer bond effectiveness, and increase shear strength (AL-Oqla *et al.,* 2022). Therefore, this study aims to determine the effect of alkaline treatment on ZMF in terms of fiber density, crystallinity index, thermal stability, scanning electron microscopy (SEM), interfacial share strength (IFSS), water absorption, tensile and flexural strength of composites. The results have significant relevance in assessing the viability of ZMF as materials for prosthetic sockets.

2. Methodology

2.1 Materials and Salacca zalacca midrib fiber treatment

Salacca zalacca midrib fiber (ZMF) aged approximately 3 years was obtained from local farmers in Wonosobo, Central Java, Indonesia. The fiber production process comprised removing the fronds' skin and soaking for 7 days. The samples were then washed with water and dried in the sun. Subsequently, ZMF was heated in an oven at 60 °C for 8 hours and stored in a moisture-proof container, followed by treatment using alkali (5% NaOH) with a soaking time of 0, 3, 6, 9, and 12 hours. The fiber was washed with distilled water until pH7 was obtained, and ZMF was copped to 10 mm lengths for composites reinforcement. NaOH was obtained from the TJ Kimia Shop, Purwokerto Indonesia. Unsaturated polyester with the Yukalac BQTN 157 Type (series) and methyl ethyl ketone peroxide (MEKPO) used as a catalyst was purchased from PT Justus Kimia Raya Semarang Indonesia. Microcrystalline cellulose (MCC) series 310697 measuring 20 micrometers with a density of 1.56 g/cm³ was obtained from PT Sigma Aldrich Jakarta, Indonesia.

a) Zalacca plant b) ZMF copped

Figure 1. *Zalacca salacca* midrib fiber and plant

2.2 Fiber and composites density

Fiber density testing was conducted based on ASTM 792-13, 2013 guidelines. The method was used with the Precisa XT 220 A Balance (Indonetwork Jakarta, Indonesia) by comparing the weight in fluids and the air using the formula below:

$$\rho = \frac{W_1}{W_o + W_1} x \rho a \quad 1)$$

ρ = composite density gram/cm³
W_1 = mass of composite in air (gram)
W_o = mass of composite in water (gram)
ρa = density of water in the room temperature 0.9978 gram/cm³

2.3 X-Ray diffraction

An x-ray diffraction test of ZMF in the cellulose structure was measured at room temperature and carried out at the Integrated Laboratory of Diponegoro University, Semarang, Indonesia. X-ray diffraction used CuK radiation or n = 1.54 A, and the radiation intensity was recorded from 2 theta = 1000 in 2 theta steps with a voltage of 30 kV and a current of 30 mA. The calculation of crystallinity index (Cr. I) and degree of crystallinity (%) were carried out using the Segal method, as shown in the equation below:

$$\text{Cr. I} = \frac{I_{(002)} - I_{am}}{I_{(002)}} \times 100\% \quad 2)$$

The peak sample intensity was carried out based on the Miller index (002) with 2 theta angles, which ranged from 22 to 23 degrees. The intensity of the non-crystalline content was at the peak angle of 2 theta = 18 degrees.

2.4 Thermogravimetry (TGA) analysis

TGA analysis was performed using the Perkin Elmer Pyris diamond TGA 6 analyzer model at the Integrated MIPA Laboratory, Sebelas Maret University, Surakarta, Indonesia. The analysis comprised subjecting all ZMF samples to scanning at room temperature, which increased from 30 °C to 600 °C in the range of 100 °C/minute. In addition, TGA test was carried out in a nitrogen environment.

2.5 Interfacial shear strength (IFSS) and single fiber pull out

Interfacial shear strength (IFSS) test was carried out by attaching 60 mm long ZMF to a mixture of MCC, unsaturated polyester (UPRs), and Mekpo. The samples were then attached to a cardboard with a hole in the middle and dried for 120 minutes. ZMF had a diameter of 5 - 10 µm, the clamping distance from the hole was 50 mm with a tensile speed of 250 mm/minute, and the single fiber tensile test was repeated 30 times. The paper from both sides of the hole was cut for maximum traction, and ZMF was pulled until it was released from the Matrix. The diameter was measured at the top, middle, and bottom sides. The test used a textile pulling machine model Tenso 300 with a type E Newton unit at the Textile Laboratory of the Indonesian Islamic University Yogyakarta.

2.6 Composites fabrication

Composites fabrication began by cutting 10 mm long ZMF and placed randomly on

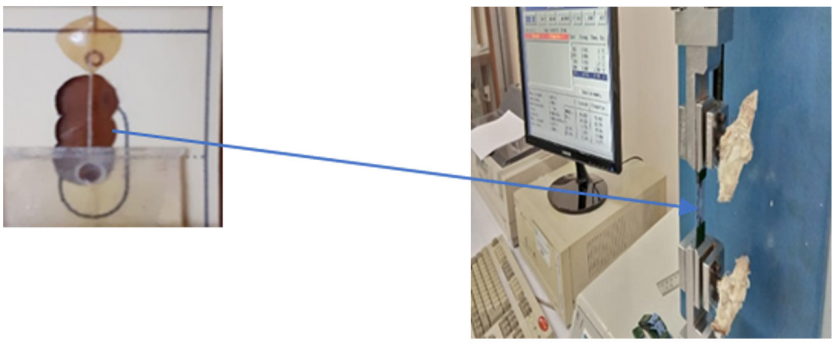

Figure 2. IFFS and tensile strength single fiber test

the mold. The products were made with variations of 60% matrix, 30% fiber, and 10% MCC. The unsaturated polyester was mixed with MCC in a container and spun at 250 rpm and 40 °C for 30 minutes. The mixture of matrix and MCC was then added with a 1% MEKPO catalyst and placed into a mold using a vacuum infusion system. Composites mold obtained was placed in an oven at 60 °C for 120 minutes before cutting the specimen.

2.7 Tensile, flexural strength, and modulus elasticity

The ASTM D638-03 (2003) standard was used to test the tensile strength of composites and the ASTM D790-03 (2003) standard was used to assess flexural strength. The procedures were carried out using a Universal Testing Machine (UTM) produced by the SANS Testing Machine Co., Ltd series 4160 (Guangzhou China). The tensile and flexural strength tests were carried out at the Materials Laboratory of Sebelas Maret University, and the specimen test was performed 5 times.

2.8 Scanning electron microscopy (SEM)

An SEM test was performed using the instrument model JSM-610 PLUS/LV from JEOL. The test was used to capture 2-dimensional images of untreated and base-treated composite fractures at the MIPA Integrated Laboratory, State University of Malang. The small dimension composites were mounted on a platinum-coated aluminum sheet and observation was carried out carefully for 1 minute at a pressure of 2 bar.

2.9 Finite element analysis (FEA)

Based on the results on tensile and flexural strength of composites, along with modulus of elasticity and density, the data for Finite Element Analysis (FEA) design used findings with the highest composites strength.

3. Results and Discussion

3.1 Fiber density and composites density

The density test of untreated and treated *Salacca zalacca* midrib fiber (ZMF), as well as the density test of composites reinforced with microcrystalline cellulose (MCC) and treated and untreated ZMF, are presented in Table 1.

The density test results showed that the fiber after treatment (ZFT) experienced an increase in weight compared to the pre-treatment value (ZFUT). After 9 hours of soaking (ZFT 9), the parameter increased from 1.27 to 1.36 gram/cm3. The expansion in ZMF density was in line with the length of immersion time and the concentration of NaOH (Makhlouf *et al.,* 2022). This was due to the loss of impurities and low-density amorphous components (Singh *et al.,* 2021). Subsequently, alkali treatment led to the formation of a more stable and compact cellulose II structure compared to cellulose I (Ibrahim *et al.,* 2022). A similar increase of ± 30% in fiber density due to alkaline treatment was observed in flax, borassus, and cantala (Hamciuc *et al.,* 2022). Composites density increased in line with increasing fiber density (ZMF). The untreated fiber had a density of 1.34 g/cm³ and the 9-hour alkali treatment increased to 1.47 g/cm³. After 12 hours of alkali treatment, the value decreased due to the polymorphic transformation of cellulose-1-to-cellulose-2. The transformation reduced the area of the crystal fiber, leading to a decrease in density (Bouramdane *et al.,* 2022). The hemp fiber-reinforced composites with a resin matrix produced a density of 1.3 - 1.5 g/cm³. (More, 2022).

Table 1. Fiber density

No.	Code	Description	Density fiber (g/cm³)	Density Composite (g/cm³)
1	ZFUT	Fiber Untreated - Composite	1.27	1.34
2	ZFT3	Fiber treated 3 h - Composite	1.31	1.38
3	ZFT6	Fiber treated 6 h - Composite	1.33	1.45
4	ZFT9	Fiber treated 9 h - Composite	1.36	1.47
5	ZFT12	Fiber treated 12 h - Composite	1.34	1.46

The addition of MCC to composites had a density effect because the value became higher, thereby reducing the cavity area that must be filled by matrix or fiber (Abbas *et al.,* 2022).

3.2 X-Ray diffraction

Figure 2 showed that ZMF was formed with 3 peaks, namely 15.2., 22.12., 44°. The first peak was in the crystal field 110 and 002 (Montoya *et al.,* 2022), and the peak in 040 was the final diffraction peak in plant fiber in the crystal field (Bouramdane *et al.,* 2022).

The cellulose structure was visible between 22 and 23° showing the original form. ZMF structure on the diffractogram in both valleys at theta was approximately 18°, and x-ray diffraction at the highest and lowest intensities was shown in Figure 3. The untreated fiber (ZFUT) exhibited a cellulose structure at a diffraction angle of 21.24° with an intensity of 1176, while the amorphous or valley portion appeared at 18.68° of diffraction with a crystallinity index of 50.97 %. After the ZFT3 treatment, a diffracted cellulose structure emerged at an angle of 22.66°with an intensity of 2242. The amorphous was observed at an angle of 18.84° with an intensity of 639 and a crystallinity index of 60.48%. Subsequent treatments, such as ZFT6 and ZFT9 showed higher crystallinity indexes of 62.62% and 63.87%, respectively. The decrease in the crystallinity index occurred in ZFT12 with a crystallinity index of 60.25%. The x-ray diffraction test showed that the alkaline treatment could increase the crystallinity index by 12.9%.

An increase in the crystallinity index indicated that the arrangement of polymer chains in the material was regular or the crystal parts were perfect and there was a decrease in the amorphous fiber composition (Perera *et al.,* 2022). Subsequently, the partial removal of binding agents, such as lignin led to the transformation of form I to form II cellulose chains (Lee *et al.,* 2021).

3.3 TGA analysis and derivative TGA

The results of TGA and derivative TGA tests are shown in Figure 4a and 4b as a basis for conducting the analysis.

Evaporation of water that occurred at temperatures between 30 and 200 °C was called desorption. Based on Figure 4a and Table 2, the results obtained from fiber without treatment showed a weight loss of 7.68% at a temperature below 100 °C. Alkaline ZFT3 exhibited a reduction of 6.78% and experienced a weight reduction of 5.86 after 12 hours. The test findings showed that the alkali treatment of fiber could reduce desorption.

The second stage of decomposition occurred at temperatures between 200 and -400 °C, along with the degradation of hemicellulose and some lignin (Ariawan *et al.,* 2020). Fiber decomposed at a temperature of 267.53 °C, with a weight reduction of 58.34%. The peak decomposition occurred at a temperature of 269.34 °C.

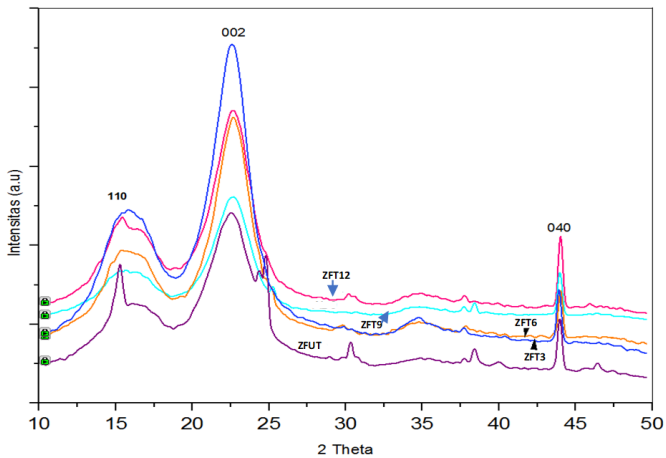

Figure 3. X-ray diffraction test

A weight loss of 54.78% occurred at ZFT3 and decreased on ZFT9 at a range of 50.36 %. Meanwhile, for ZFT12, decomposition occurred at a temperature of 276.87 °C, leading to a weight loss of 50.91%. The ZMF degradation before and after alkali treatment showed that there was an increase in the value of thermal stability due to the loss of hemicellulose, lignin, and pectin in fiber (Amjad *et al.,* 2022).

The third decomposition stage was related to the degradation of hemicellulose and lignin. ZFUT fiber exhibited a weight loss of 14.45% during decomposition, while fiber treated with ZFT12 experienced a weight loss of 9.67%.

The DTGA graph (Figure 4b) showed the peak in the desorption of water absorption at To, T2 degradation of hemicellulose, and the peak position of T3 degradation of lignin (Lee *et al,* 2021). The results of the DTGA graph are presented in Table 3.

The residue of untreated fiber showed a smaller amount compared to the post-treatment sample. Fiber residue without treatment was 21.04%, while after 9 hours of alkaline treatment, a value of 29.82% was obtained.

3.4 Interfacial shear strength (IFSS) and tensile strength single fiber

The tensile strength test was observed in fiber before treatment, while the highest tensile strength was recorded after soaking for 9 hours. The results of the Interfacial Shear Strength (IFSS) test for untreated ZMF showed a value of 0.48 MPa. The increase in shear force occurred in ZFT3 of 0.77 MPa and the highest test results were obtained in ZFT9 of 1.09 MPa, as shown in Table 4.

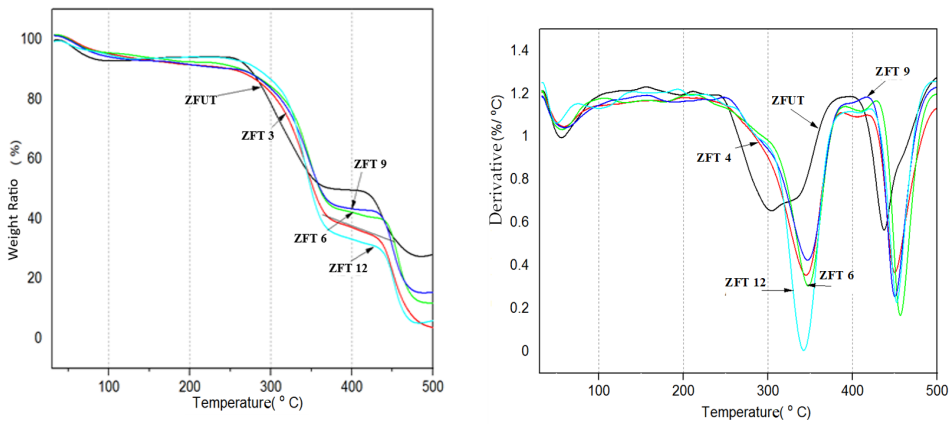

Figure 4. Thermogravimetric analysis (TGA) and derivative TGA

Table 2. TGA analysis

Code	30 - 200 °C Final Temp/wt. loss (%)	200 - 400 °C Initial Temp/wt. loss (%)	400 - 600 °C Initial Temp/wt. loss (%)
ZFUT	88.82/7.68	267.53/58.34	424.45/14.45
ZFT3	92.81/6.78	269.34/54.78	419.23/12.45
ZFT6	94.43/6.18	271.45/53.12	427.85/10.83
ZFT9	95.84/5.82	273.43/50.36	418.34/9.39
ZFT12	98.38/5.86	276.87/50.91	414.56/9.67

Table 3. Derivative TGA alkali treatment

Treatment	To (°C)	T2 (°C)	T3 (°C)	Residue
ZFUT	55. 10	354.21	437.34	21.04
ZFT3	58.67	364.91	464.08	25.23
ZFT6	58.93	354.78	467.06	27.54
ZFT9	60.43	359.98	478.34	29.82
ZFT12	58.78	354.23	474.92	26.82

The tensile strength and IFSS of ZMF increased significantly after alkaline treatment (Jamadi *et al.,* 2021). The results showed that the alkaline treatment hardened the surface of the fiber due to the reduction in hemicellulose, lignin, wax, and pectin. This alteration contributed to the improved interfacial tensile strength between ZMF and the matrix (Muralidharan, 2022). The increase in tensile strength and IFSS was directly proportional to the increase in the crystallinity index on fiber from the x-ray diffraction test.

3.5 Tensile strength and flexural composite

The results of the tensile and flexural strength tests of ZMF and MCC reinforced composites are presented in Figures 5a and 5b.

The tensile strength of composites experienced a substantial increase, reaching 44.28 Mpa, following ZFT9. The increase in the tensile strength of composites was due to the interfacial bond strength between fiber and the matrix. This was also due to the MCC mixture, which was pure cellulose. Subsequently, MCC could fill micro holes in the composites, thereby leading to an increase in the strength (Yorseng *et al.,* 2022). After ZFT9, the tensile strength decreased due to the long soaking time, which affected ZMF defibrillation (Bachchan *et al.,* 2022). The results showed that the graphs of tensile and modulus tests had almost the same outcome (Selvaraj *et al.,* 2022).

Figure 5b showed that the flexural strength of the untreated composite reinforced with ZMF was 31.45 MPa, but significantly rose to 56.28 MPa after ZFT9. The yield of flexural strength was higher than the composite reinforced with kenaf fiber and the epoxy matrix (Almeida *et al.,* 2022). The parameter could be attributed to ZMF purification through alkali treatment, eliminating amorphous components, such as hemicellulose, pectin, and lignin. In addition, the incorporation of MCC, such as pure cellulose, contributed to the improved strength by closing voids. Test results, as depicted in the graphs and modulus of elasticity, correlated with the observed flexural strength (Sun *et al.,* 2022).

3.6 SEM observation

The fracture of the tensile strength test results for ZMF and MCC reinforced composites was observed by SEM, as shown in Figure 6.

Table 4. Test results for single fiber tensile strength and IFSS

Treatment	Tensile (Mpa)	Modulus elasticity (GPA)	IFSS (MPa)
ZFUT	111.81 ± 17.87	93.56 ± 22.34	0.48 ± 0.21
ZFT3	253.98 ± 29.65	148.18 ± 34.91	0.77 ± 0.31
ZFT6	271.81 ± 39.91	176.68 ± 37.24	1.07 ± 0.39
ZFT9	288.81 ± 42.92	201.34 ± 46.17	1.09 ± 0.41
ZFT12	273.81 ± 40.93	186.34 ± 37.28	1.03 ± 0.28

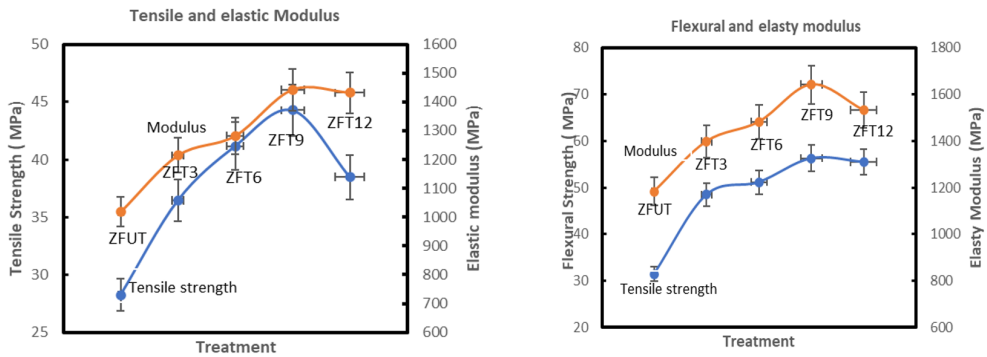

a) Tensile and elastic modulus b) Flexural and elastic modulus

Figure 5. Tensile, flexural strength, and elastic modulus

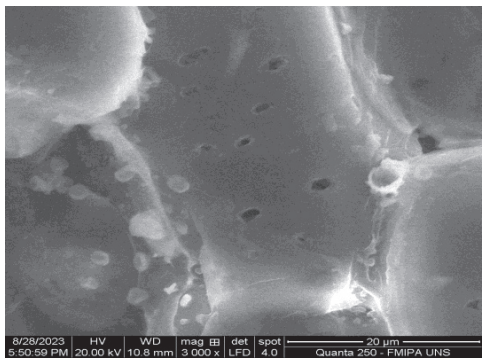

a) SEM – ZFUT fiber

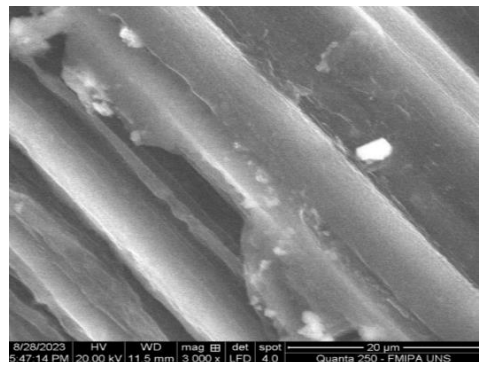

b) SEM ZFT9

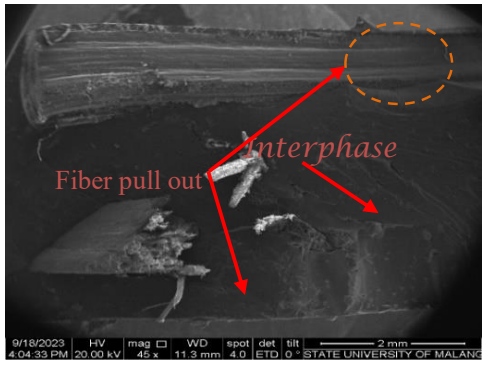

c) SEM - ZFUT composite

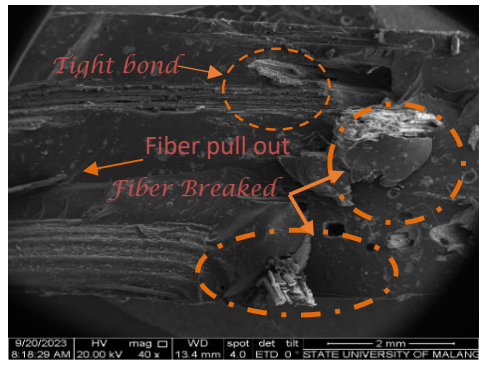

d) SEM – ZFT9 composite

Figure 6. Scanning electron microscopy (SEM) fiber and composite

The results of SEM observation of ZMF showed that before treatment, fiber exhibited a network structure with bound fibrils and was covered with other substances, including pectin, lignin, hemicellulose, and other substances. The unprocessed fiber contained impurities, wax, fatty substances, and rounded protrusions known as "tylose" (Asyraf *et al.,* 2022). After a 9-hour alkaline treatment, the sample showed a cleaner appearance as the cement-like substances started to disappear. This cleansing effect was due to the removal of hemicellulose, pectin, wax, oil, and other extractive substances. The alkaline treatment of ZMF significantly smoothed the surface of ZMF by eliminating dirt, fat deposits, and wax (Ariawan *et al.,* 2020)

The results of observations of untreated fiber composites showed smoothness, with several interphase gaps and the sample was dominated by pulled fiber. Interphase was caused due to the presence of hemicellulose, lignin, pectin, and other impurities. The interface in the composite was caused by differences between the hydrophobic properties of the polymer and the hydrophilic properties of natural fiber, leading to poor mechanical interlocking and tensile fracture (Zheng *et al.,* 2023).

In Figure 5d, the SEM morphological results of ZFT9-reinforced composites showed that fiber degraded under interphase conditions with strong bonds due to the reduced hemicellulose, pectin, and lignin content. The loss of amorphous in ZMF due to alkaline treatment led to a coarser fiber and increased interfacial bonding, causing an optimal transfer from matrix to fiber and increased strength.

The addition of MCC to the composite led to the closure of the cavities due to its small size, leading to an increase in the strength. MCC in the composite produced a smooth surface structure due to the microparticle size.

3.7 Water absorption in composites

The water absorption test for ZMF reinforced composites and MCC is presented in Figure 7.

The test results showed that the penetration of water into composites caused the formation of a linear graph during the first week of immersion and started to slow down by the third week. Water absorption reached a state of equilibrium between 30 days of immersion, with absorption rates tapering off as the sample approached saturation. This water absorption behavior was consistent with the Fickian model and diffusion process (Hernández *et al.,* 2020), characterized by rapid water absorption, followed by saturation at the next absorption step (Deeban *et al.,* 2023). The removal or reduction of hemicellulose and lignin in ZMF after alkaline treatment had been proven by density, x-ray, TGA, tensile, flexural, SEM, and IFSS tests, indicating that ZFT9 gave the best outcome.

3.8 ZMF as a prosthetic socket reinforcement

United States Department of Veterans carried out a comparative investigation of the tensile strength of materials for the manufacture of prosthetic sockets from various companies. These included IPOS, Bauerfeind Prosthetic, USA, Kennesaw, Ottobock, Healthcare, Minneapolis, Orthopedic products, and others (Barrios-Muriel *et al.,* 2020), as shown in Figure 8

The results of the tensile strength test of the composite reinforced with ZMF and MCC showed that the highest value for the alkaline treatment was 44.28 MPa. This value was higher than the tensile strength of perlon, nylon, cotton, and spectralon. Consequently, composite materials reinforced from ZMF and MCC were suitable for use in prosthetic sockets due to their impressive tensile strength performance.

The tensile strength test results were applied using Finite Element Analysis (FEA), which showed the highest stress of 6.531 MPa with a load of 700 Newtons. This indicated that the use of ZMF was very safe when used for prosthetic sockets.

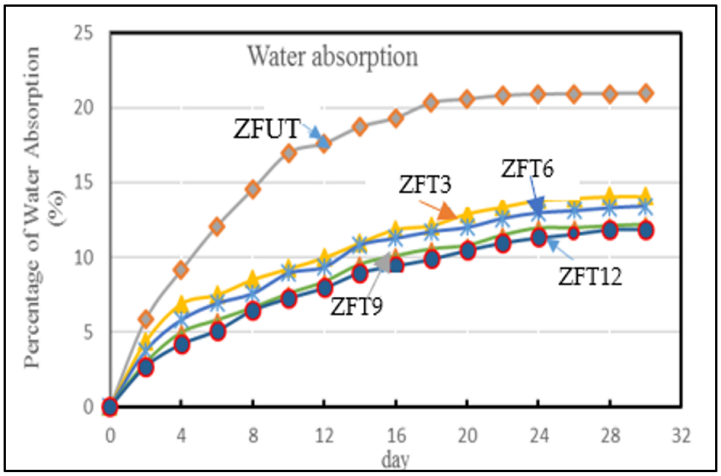

Figure 7. Water absorption on composites

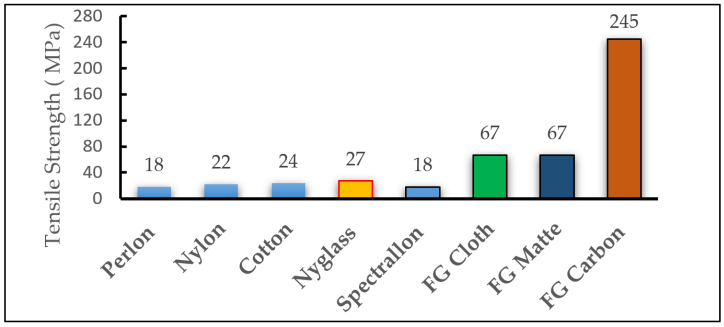

Figure 8. Ottobock type tensile strength of various materials

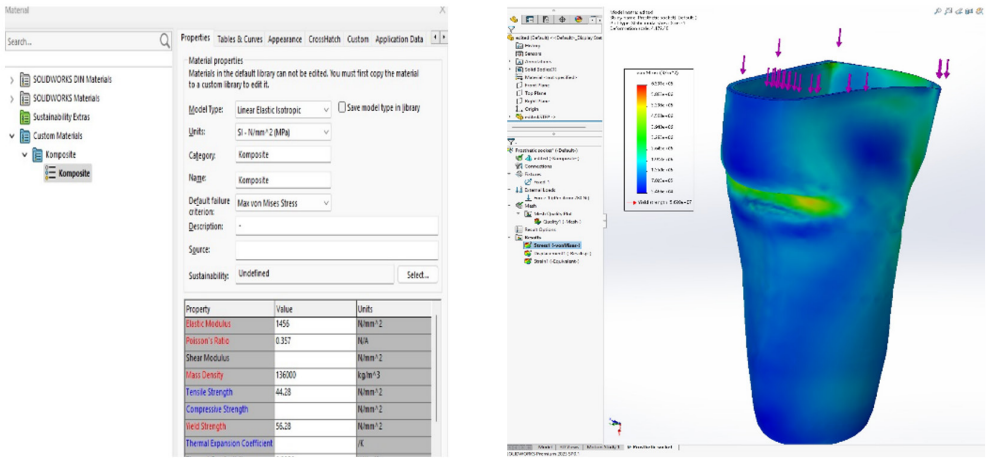

Figure 9. Finite element analysis (FEA) prosthetic sockets

4. Conclusion

In conclusion, the alkaline treatment of *Salacca zalacca* midrib fiber (ZMF) led to an increase in fiber density due to the loss of some amorphous components in fiber. An increase in the crystallinity index in the alkaline treatment indicates a decrease in the amorphous fiber composition. In addition, fiber treated with alkali had a better thermal stability. The interfacial bonding between fiber after alkaline treatment showed an increase due to a decrease in hemicellulose, pectin, lignin, and other impurities. After alkaline treatment for 9 hours, the sample showed a cleaner appearance as the cement-like substances started to disappear. The cleansing effect was due to the removal of hemicellulose, pectin, wax, oil, and other extractive substances. The alkaline treatment of ZMF significantly smoothened the surface of ZMF by eliminating dirt, fat deposits, and wax. The improvement extended to the physical and mechanical properties of composites, which were further aided by the addition of microcrystalline cellulose (MCC). The results of water absorption showed that fiber experienced a decrease after being treated with alkali. The findings of the tensile strength test showed that the bark fiber and MCC could be used as prosthetic sockets materials.

Acknowledgment

The authors are grateful to the Directorate of Research for Technology and Community Service (DRTPM) of the Ministry of Education and Culture of Indonesia for providing fundamental study funding in 2023.

References

Abbas AGN, Aziz FNAA, Abdan K, Mohd Nasir NA, Norizan MN. Kenaf fibre reinforced cementitious composites. Fibers 2022;10 (3): 1-24.

Al-Oqla FM, Hayajneh MT, Al-Shrida MAM. Mechanical performance, thermal stability and morphological analysis of date palm fiber reinforced polypropylene composites toward functional bio-products. Cellulose 2022; 29(6): 3293-3309.

Almeida NCE, Valle V, Aguilar A, Cadena F, Kreiker J, Raggiotti B. Water absorption behavior of oil palm empty fruit bunch (OPEFB) and oil palm kernel shell (OPKS) as fillers in acrylic thermoplastic composites. Materials 2022;15(14): 1-17.

Amjad A,,Abidin MSZ, Alshahrani H, Rahman AA. Effect of fibre surface treatment and nanofiller addition on the mechanical properties of flax/PLA fibre reinforced epoxy hybrid nanocomposite. Polymers 2021; 13(21): 1-12.

Ariawan D, Rivai TS, Surojo E, Hidayatulloh S, Akbar HI, Prabowo AR. Effect of alkali treatment of *Salacca zalacca* fiber (SZF) on mechanical properties of HDPE composite reinforced with SZF. Alexandria Engineering Journal 2020; 59(5): 3981-3989.

Asyraf MR, Ishak MR, Syamsir A, Nurazzi NM, Sabaruddin FA, Shazleen SS, Razman MR. Mechanical properties of oil palm fibre-reinforced polymer composites: A review Journal of Materials Research and Technology 2022; 17 (1): 33-65.

Barrios MJ, Romero SF, Alonso SFJ, Salgado DR. Advances in orthotic and prosthetic manufacturing: A technology review. Materials 2020; 13(2): 295-309.

Bachchan AA, Das PP, Chaudhary V. Effect of moisture absorption on the properties of natural fiber reinforced polymer composites: A review Materials Today Proceedings 2022; 49 (4) : 3403-3408.

Bouramdane Y, Fellak S, El Mansouri F, Boukir A. Impact of Natural Degradation on the Aged Lignocellulose Fibers of Moroccan Cedar Softwood: Structural Elucidation by Infrared Spectroscopy (ATR-FTIR) and X-ray Diffraction (XRD). Fermentation, 2022; 8(12): 698-706.

Deeban B, Maniraj J, Ramesh M. Experimental investigation of properties and aging behavior of pineapple and sisal leaf hybrid fiber-reinforced polymer composites. e-Polymers, 2023;23(1): 1-11..

Hafidz NBM, Rehan MBM, Mokhtar HB. Effect of alkaline treatment on water absorption and thickness swelling of natural fibre reinforced unsaturated polyester composites. Materials Today: Proceedings 2022; 48(8): 720-727.

Hakim L, Widyorini R,Nugroho WD, Prayitno TA. Effect of vascular tissue on mechanical properties of fibrovascular bundles of Salacca sumatrana Becc. fronds. Journal of Natural Fibers 2022; 19(14): 9335-9347.

Hamciuc C, Vlad BT, Serbezeanu D, Macsim AM, Lisa G, Anghel I, Şofran IE. Effects of phosphorus and boron compounds on thermal stability and flame retardancy properties of epoxy composites. Polymers 2022; 14(19): 40-55.

Hernández DD, Villar RR, Espinach FX, Julián F, Hernández AV, Delgado AM. Impact properties and water uptake behavior of old newspaper recycled fibers-reinforced polypropylene composites. Materials 2020; 13(5): 10-27.

He L, Xia F, Wang Y, Yuan J, Chen D, Zheng J. Mechanical and Dynamic Mechanical Properties of the Amino Silicone Oil Emulsion Modified Ramie Fiber Reinforced CompositesJ. Polymers 2021; (13):40-53.

Ibrahim YE, Adamu M, Marouf ML, Ahmed OS, Drmosh QA, Malik MA. Mechanical performance of date-palm-fiber-reinforced concrete containing silica fume. Buildings 2022; 12(10): 1-20.

Ihueze,CC, Okafor CE, Obuka SN, Abdulrahman J, Onwurah UO. Integrity and cost evaluation of natural fibers/HDPE composite tailored for piping applications. Journal of Thermoplastic Composite Materials 2021; 36(1): 372-398.

Ilyas RA, Zuhri MYM, Aisyah HA, Asyraf MRM, Hassan SA, Zainudin ES, Sari NH. Natural fiber-reinforced polylactic acid, polylactic acid blends and their composites for advanced applications. Polymers 2022; 14(1): 202-216.

Iwasaki KM, Reis PA, De Medeiros. Angustifolia fibre composite extracted via rotary–peeling method. Journal of the Brazilian Society of Mechanical Sciences and Engineering 2022; 44(4): 135-144.

Jamadi AH, Razali N, Petrů M, Taha MM, Muhammad N, Ilyas RA. Effect of chemically treated kenaf fibre on mechanical and thermal properties of PLA composites prepared through fused deposition modeling (FDM). Polymers 2021; 13(19): 329-339.

Lee CH, Khalina A, Lee SH. Importance of interfacial adhesion condition on characterization of plant-fiber-reinforced polymer composites: A review. Polymers 2021; 13(3): 438-447.

Makhlouf A, Belaadi A, Amroune S, Bourchak M, Satha H. Elaboration and characterization of flax fiber reinforced high density polyethylene biocomposite: effect of the heating rate on thermo-mechanical properties. Journal of Natural Fibers 2022; 19(10): 3928-3941.

Muralidharan D. Mechanical characteristics study of chemically modified kenaf fiber reinforced epoxy composites. Journal of Natural Fibers 2022; 19(7): 2457-2467.

Oleiwi JK, Hamad QA, Faheed NK. Experimental, Theoretical, and Numerical Analysis of Laminated Composite Prosthetic Socket Reinforced with Flax and Cotton Fibers. Biotribology 2023; 35(36): 102-114.

Perera HJ, Goyal A, Alhassan SM . Morphological, structural and thermal properties of silane-treated date palm fibers. Journal of Natural Fibers 2022; 19(15): 12144-12154.

Sakuri S, Surojo E, Ariawan D, Prabowo AR.Experimental investigation on mechanical characteristics of composite reinforced cantala fiber (CF) subjected to microcrystalline cellulose and fumigation treatments. Composites Communications 2020; 21(20): 1-21.

Sakuri S, Susanto TD, Sugiantoro, B.Experimental Investigation of Hot Alkaline Treatment on Strength Characteristics of Cantala Fiber Reinforced Composites and Microcrystalline Cellulose. EnvironmentAsia 2023;16(1): 146 -156.

Sakuri S, Surojo E, Ariawan D, Prabowo AR. Investigation of Agave cantala-based composite fibers as prosthetic socket materials accounting for a variety of alkali and microcrystalline cellulose treatments. Theoretical and Applied Mechanics Letters 2020;10(6): 405-411.

Sakuri S, Surojo E, Ariawan D. Optimization of mechanical properties of unsaturated polyester composites reinforced by microcrystalline cellulose various treatments using the Taguchi method. Springer Singapore 2020,12(1) : 225-231.

Seal B, Chaudhary V, Sadhu SD. Development of natural fiber reinforced nanocomposites: Future Scope, challenges, and applications. Materials Today: Proceedings 2023; 78(1): 614-619.

Selvaraj G, Kaliyamoorthy R, Kirubakaran R. Mechanical, thermogravimetric, and dynamic mechanical analysis of basalt and flax fibers intertwined vinyl ester polymer composites. Polymer Composites 2022; 43(4): 2196-2207.

Singh JK, Rout AK, Kumari K. A review on Borassus flabellifer lignocellulose fiber reinforced polymer composites. Carbohydrate Polymers 2021;262 (1): 117-129.

Sun SF, Yang HY, Yang J, Shi ZJ. The effect of alkaline extraction of hemicellulose on cocksfoot grass enzymatic hydrolysis recalcitrance. Industrial Crops and Products 2022; 178(1): 144-154.

Yorseng K, Rangappa SM, Parameswaranpillai J, Siengchin S..Towards green composites: Bioepoxy composites reinforced with bamboo/basalt/carbon fabrics. Journal of Cleaner Production 2022; 363(1): 132-144 .,

Zheng Z, Wu Z, Zhao R, Ni Y, Jing X, Gao S. A review of EMG-, FMG-, and EIT-based biosensors and relevant human–machine interactivities and biomedical applications. Biosensors 2022; 12(7): 516-529.